Journal of Alloys and Compounds 509 (2011) 2627–2630

Contents lists available at ScienceDirect

Journal of Alloys and Compounds

journal homepage: www.elsevier.com/locate/jallcom

Low temperature fabrication of nano-structured porous LSM–YSZ composite cathode film by aerosol deposition

Jong-Jin Choi[a,*], Sung-Hoon Oh[a], Ho-Sung Noh[b], Hae-Ryoung Kim[b], Ji-Won Son[b], Dong-Soo Park[a], Joon-Hwan Choi[a], Jungho Ryu[a], Byung-Dong Hahn[a], Woon-Ha Yoon[a], Hae-Weon Lee[b]

[a] Functional Ceramics Group, Functional Materials Division, Korea Institute of Materials Science, 797 Changwondaero, Changwon, Gyeongnam 641-831, Republic of Korea
[b] High-Temperature Energy Materials Center, Korea Institute of Science and Technology, P.O. Box 131, Cheongryang, Seoul 130-650, Republic of Korea

ARTICLE INFO

Article history:
Received 6 October 2010
Received in revised form
15 November 2010
Accepted 19 November 2010
Available online 1 December 2010

Keywords:
Aerosol deposition
LT-SOFC
LSM–YSZ
Nano-structure
Low temperature process

ABSTRACT

A low temperature (≤500 °C) process for fabricating nano structured porous LSM–YSZ composite films, ~35 μm in thickness, for use as a cathode in the low temperature solid oxide fuel cell (LT-SOFC) was developed using a ceramic–polymer composite powder and an aerosol deposition (AD) process. Polyvinylidene fluoride (PVDF) polymer powder was mixed with LSM and YSZ ceramic powders, as a pore former to prepare the composite powder for AD. The deposited LSM–YSZ composite ceramic film maintained good adhesion with the YSZ electrolyte and showed >40% porosity with a particle and pore size of 10–100 and 100–200 nm, respectively. The peak power density of the YSZ electrolyte-based, anode-supported-type cell with the nano-structured LSM–YSZ cathode produced by AD was 140 mW/cm^2 at 600 °C.

1. Introduction

One of the critical challenges in the commercialization of solid oxide fuel cells (SOFCs) is to develop cells that can operate at sufficiently low temperatures to reduce the cost and improve the reliability [1]. Among the parts of a SOFC stack, the cathode plays an important role because most of the power losses arise from the cathode relevant to oxygen reduction, particularly at lower operation temperatures [2,3]. Strontium-doped lanthanum manganite (LSM) is one of the most widely used cathode materials owing to its high electrochemical activity for oxygen reduction, good stability and compatibility with the yttria stabilized zirconia (YSZ) electrolyte. However, the oxygen conductivity of LSM materials is inadequate at low temperatures. Therefore, a material with high ionic conductivity (i.e. YSZ) is added to form a composite material with high ionic and electronic conductivity. In this case, the oxygen reduction reaction site can be extended from the cathode/electrolyte interface to inside the composite cathode due to an enlargement of the electrochemically active triple phase boundary (TPB), where electrons, oxygen ions, and oxygen gas coexist. The LSM–YSZ composite cathode have demonstrated better performance than those composed of only LSM [4,5].

The performance of the composite cathode depends strongly on the microstructure because the cathode microstructure affects the TPB distribution and site density. The TPB density can be increased using nanoparticle-based cathode materials due to the increased particle-to-particle contact points [6,7]. However, there is a limitation to decreasing the particle size using conventional sintering processes because the particle size will increase during sintering at high temperature (>1000 °C), even if a powder with an extremely small particle is used. Furthermore, conventional sintering method cannot be used for the LSM–YSZ cathode in a metal-supported type SOFC because the cathode fabrication temperature is limited by oxidation of the metal substrate [8].

The aerosol deposition (AD) process is a room-temperature operating powder consolidation method for the formation of thick and dense ceramic layers based on the impact adhesion of fine particles [9,10]. The AD process has a high potential for using in cathode fabrication due to its high deposition rate (>5 μm/min), and low processing temperature because almost full densification (>95%) with a high adhesion strength (>30 MPa) can be achieved at room temperature. In addition, the process is suitable for the formation of nano-particulate interconnected microstructures because the film consolidated by the AD process has an extremely small crystalline size, generally ranging from 5 to 20 nm. In this study, nano-structured porous LSM–YSZ composite films were deposited on the silicon and anode-supported type cells by an AD process using polyvinylidene fluoride (PVDF) as a pore former. Microstructural

* Corresponding author. Tel.: +82 55 280 3371; fax: +82 55 280 3392.
E-mail address: finaljin@kims.re.kr (J.-J. Choi).

0925-8388/$ – see front matter © 2010 Elsevier B.V. All rights reserved.
doi:10.1016/j.jallcom.2010.11.169

observations of the composite cathode and related electrochemical analysis were performed.

2. Experimental procedure

The starting powders were commercially available LSM ($La_{0.8}Sr_{0.2}MnO_3$, LSM20-P, Fuelcellmaterials, OH) and YSZ ($(Y_2O_3)_{0.08}(ZrO_2)_{0.92}$, FYT13.0-010H, Unitec Ceramics, UK) powders. Polyvinylidene fluoride (PVDF) polymer powder (99.9% purity, Aldrich Co., Milwaukee, WI) was used as the pore former. The oxide powders were mixed at a 6:4 volume ratio. PVDF powder was then added to the mixed LSM–YSZ powder at a volume ratio of 0–50%. The mixed powder was ball-milled for 6 h in a nylon jar using zirconia balls as the milling media and ethanol as the solvent, and dried at ~80 °C to obtain a submicron-sized powder suitable for film deposition.

A schematic diagram of the AD equipment is reported elsewhere [11]. The dried, ceramic–polymer composite powders were mixed with the carrier gas to form an aerosol flow in the aerosol chamber. The aerosol flow was transported through a tube to a nozzle, accelerated and ejected into the deposition chamber through a $25 \times 0.8\ mm^2$ rectangular shaped nozzle, which was evacuated using a rotary pump with a mechanical booster. Compressed air dried through a dehumidifying filter was used as the carrier gas at a flow rate of 30 l/min. The accelerated LSM and YSZ particles collided with the YSZ/NiO-YSZ and silicon substrates, which were located 5 mm away from the nozzle. The area of cathode film was ~1.0 cm^2. The YSZ/NiO-YSZ substrate was a piece cut from 10×10 cm anode supported cells. A detailed procedure for YSZ/NiO-YSZ fabrication is reported elsewhere [12]. The deposited LSM–YSZ–PVDF composite films were annealed at 500 °C for 1 h to generate a porous structure by burning out the PVDF polymer. Therefore, 500 °C was the highest processing temperature for the fabrication of a porous LSM–YSZ cathode during the entire process.

The particle size distribution of the powders used for coating was characterized by a laser diffraction particle size analyzer (HELOS/BF, Sympatec GmbH, Clausthal-Zellerfeld, Germany). The crystalline phases of the LSM–YSZ powders and film coated on the silicon were examined by X-ray diffraction (XRD, D-MAX 2200, Rigaku, Tokyo, Japan). The film microstructures of the surface and the fractured cross-section were examined by scanning electron microscopy (SEM, JSM-5800, JEOL, Tokyo, Japan) and scanning transmission electron microscopy (STEM, JEM-2100F, JEOL, Tokyo, Japan) equipped with an energy dispersion X-ray (EDX) spectrometer. Porosity of the LSM–YSZ cathode film was measured from SEM micrograph using image analysis software (Image-Pro Plus, version 3.0, Media Cybernetics, L. D., Silver Spring, MD, USA). For the cell test, air and 97% H_2/3% H_2O were used as the oxidant and fuel, respectively, at a flow rate of 200 sccm. The cell test temperature range was 450–600 °C and the electrochemical cell performances were characterized using a Solartron impedance analyzer with an electrochemical interface (SI1260 and SI1287, Solartron). The frequency range for impedance analyses was 10^{-1}–10^6 Hz. The cell test configuration is reported elsewhere [13].

3. Results and discussion

The characteristics of the powder used for the aerosol flows were examined. The average particle size of LSM, YSZ, and PVDF, which was measured using a dry jet dispersion type analyzer, was 1.07, 0.93 and 3.50 μm, respectively, and that of the 3.6:2.4:4 (volume ratio) LSM:YSZ:PVDF mixed composite powder was 1.88 μm. The phase of the powder, as-deposited film on a silicon wafer, and film annealed at 500 °C were characterized by XRD (Fig. 1). All the powder and films had a perovskite LSM and stabilized cubic YSZ structures. However, the ratio of the peak intensity of LSM [1 1 0]/(LSM [1 1 0] + YSZ [1 1 1]) of the powder, as-deposited film, and annealed film were 0.53, 0.60 and 0.61, respectively, which means that the ratio of the LSM in the film is higher than that in the powder. The higher deposition rate of LSM than YSZ appears to have originated from the easy mechanical fracture of LSM than YSZ, which agrees well with a previous study [14].

The surface microstructure of the LSM–YSZ–PVDF composite film on a silicon substrate was observed by SEM (Fig. 2). Fig. 2(a)–(d) shows the microstructure of the LSM–YSZ–PVDF composite film after annealing at 500 °C with a PVDF ratio of 0, 10, 30, and 50%, respectively. Nano-sized pores were generated by the thermal decomposition of PVDF, and the porosity of the composite powder increased with increasing PVDF content. Fig. 2(e) and (f) shows the surface microstructure with a lower magnification and related EDX mapping quantify the atomic ratio of the LSM–YSZ–PVDF composite film with 40% of PVDF, respectively. The film showed a well-dispersed pore structure without large sized

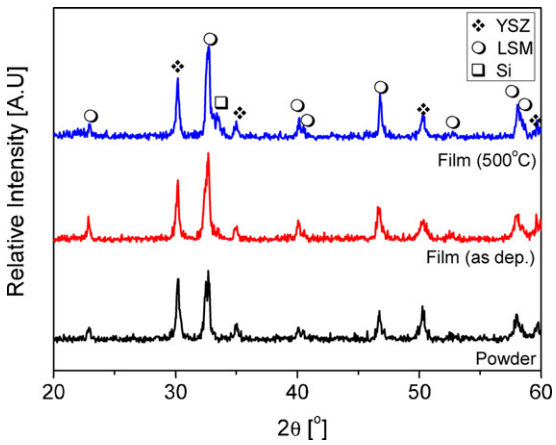

Fig. 1. XRD phase analysis; (a) LSM–YSZ composite powder, (b) LSM–YSZ composite film in the as-deposited state on silicon substrate, (c) LSM–YSZ composite film after annealing at 500 °C for 2 h.

defects, and LSM and YSZ appears to be mixed homogeneously according to EDX mapping of the Mn and Zr atoms. The volume ratio of LSM/(LSM + YSZ) in the film calculated based on the EDX quantification results was 74.7%. The ratio was higher than that in the powder (60%), which coincides with the XRD results in Fig. 1.

Fig. 3 shows the cross-sectional microstructure of the LSM–YSZ composite film with 40% PVDF on a co-fired YSZ/Ni-YSZ substrate observed by SEM and STEM. The thickness of the LSM–YSZ cathode layer was ~35 μm, and the LSM–YSZ layer showed good adhesion with the YSZ electrolyte layer, as shown in Fig. 3(a) and (b). The porosity of the composite film measured by image analysis tool from the mounted and polished cross-section was 42.1%. The particle size of the LSM–YSZ cathode layer was ~100 nm or less, as shown in Fig. 3(c) and (d), which is much smaller than the particle size of the Ni-YSZ anode functional layer (Fig. 3(b)), possibly due to the low processing temperature (500 °C). The selected area diffraction pattern (SAD) from the cathode area showed a reciprocal lattice with a ring-like pattern due to the small crystalline particles of the composite cathode.

The *I–V* characteristics with power densities and impedance spectra of the cell with the LSM–YSZ–40% PVDF composite cathode at different operation temperature up to 600 °C were analyzed. Fig. 4 and Table 1 summarize the results. The open-circuit voltages (OCV) were 1.10 V at 600 °C, and decreased with decreasing operation temperature, probably due to the sealant characteristics used for the cell test [15]. The peak power densities of the cell at 450, 500, 550 and 600 °C were 10.4, 30, 70 and 140 mW/cm^2, respectively, as shown in Fig. 4(a). It was possible to measure the cell performance down to a low temperature (450 °C). Therefore the physical structure of the AD-deposited LSM–YSZ film appears to be effective for use as a cathode in LT-SOFC. The ohmic ASR at the open cell condition and the cell ASR at 0.7 V was measured from the impedance spectra and *I–V* curves, respectively, and summarized in Table 1. Further studies will be focused on the optimization of the thickness, composition and microstructure to further enhance the cathode performance including long-term stability test.

4. Summary and conclusions

A nano-structured LSM–YSZ cathode with high adhesion strength to the electrolyte was fabricated using an AD process at low temperature (≤500 °C). The thickness and particle size of the LSM–YSZ composite cathode was ~35 μm and <100 nm, respectively. The deposited LSM–YSZ composite cathode had a higher LSM contents than the composite powder used for AD. The

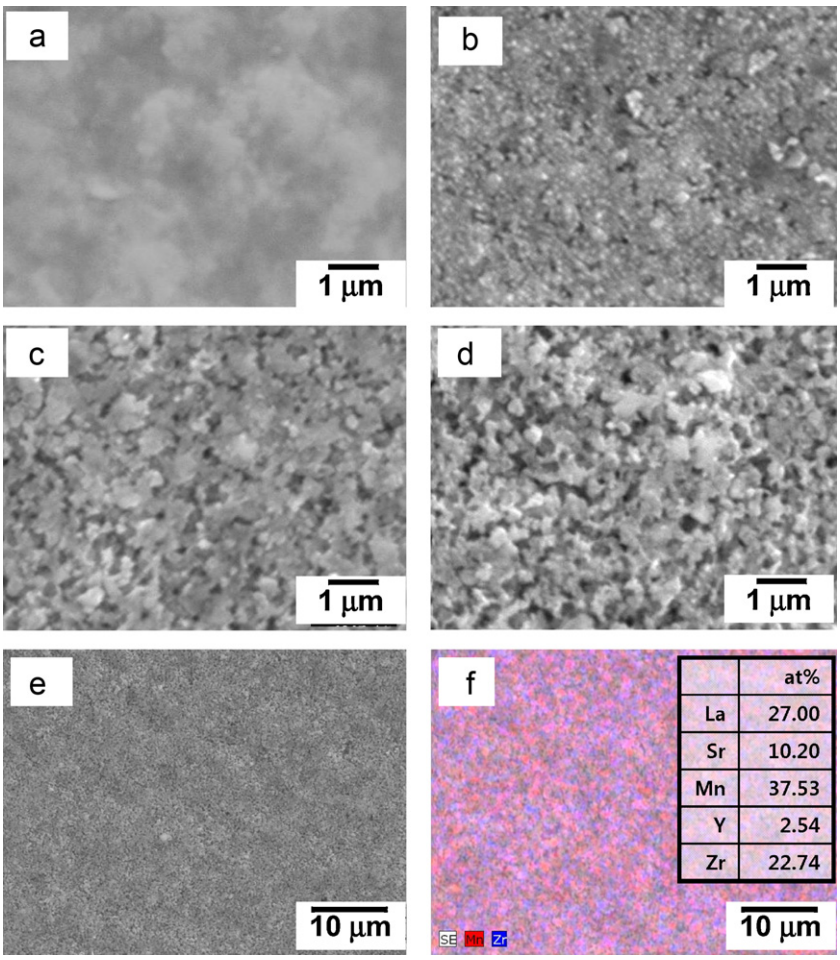

Fig. 2. SEM surface microstructures of the 500 °C-annealed LSM–YSZ composite film with different PVDF contents; (a) 0%, (b) 10%, (c) 30%, (d) 50%, (e) 40% with low magnification, and (f) EDS mapping and cation element ratio quantification of (e).

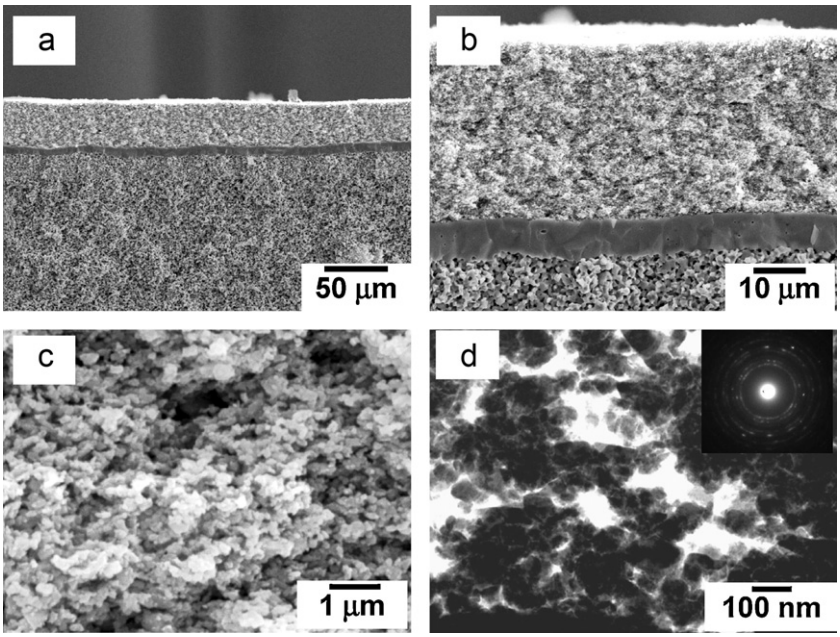

Fig. 3. (a)–(c) SEM cross-sectional microstructure of the LSM–YSZ composite cathode on co-fired YSZ/Ni-YSZ supports with different magnification. (d) STEM microstructure of the LSM–YSZ composite cathode.

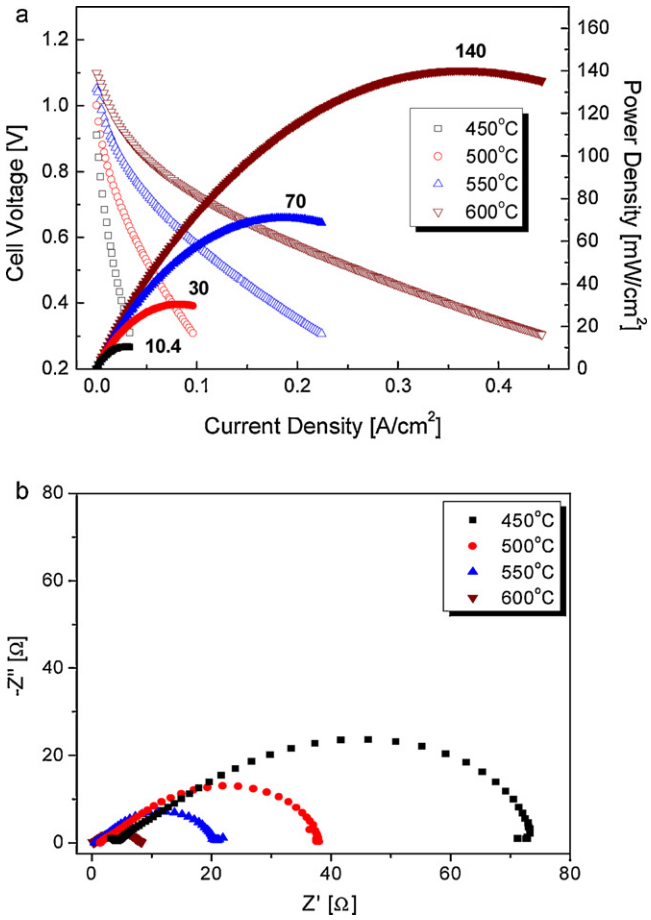

Fig. 4. (a) *I–V* characteristics and (b) impedance spectra of the cell including nano-structure LSM–YSZ composite cathode by AD with different operating temperature.

Table 1
Electrochemical performances of the cell with the nano-structure LSM–YSZ composite cathode at different operating temperatures.

Temp.	Ohmic ASR ($\Omega\,cm^2$)	Cell ASR @ 0.7 V ($\Omega\,cm^2$)	Power density @ 0.7 V (mW/cm^2)	Peak power density (mW/cm^2)
600	0.302	6.25	78.4	140
550	0.58	12	40.8	70
500	1.3	30.4	16.1	30
450	3.9	100	4.9	10.4

YSZ-electrolyte-based SOFC cell with the AD-deposited LSM–YSZ cathode showed a peak power density of 140 mW/cm^2 at 600 °C. The AD-deposited cathode has potential not only for nano structure materialization, but also for the metal-supported type SOFC where the cathode fabrication temperature is limited by oxidation of the metal substrate.

Acknowledgement

This study was supported financially by Fundamental Research Program of the Korean Institute of Materials Science (KIMS).

References

[1] S.C. Singhal, Solid State Ionics 135 (1–4) (2000) 305–313.
[2] Z. Shao, S.M. Haile, Nature 431 (7005) (2004) 170–173.
[3] C. Xia, M. Liu, Adv. Mater. 14 (7) (2002) 521–523.
[4] T. Tasi, S.A. Barnett, Solid State Ionics 93 (1997) 207–219.
[5] F. Liang, J. Chen, S.P. Jiang, B. Chi, J. Pu, L. Jian, Electrochem. Commun. 11 (2009) 1048–1051.
[6] J. Chen, F. Liang, L. Liu, S. Jiang, B. Chi, J. Pu, J. Li, J. Power Sources 183 (2008) 586–589.
[7] H.S. Song, W.H. Kim, S.H. Hyun, J. Moon, J. Kim, H.-W. Lee, J. Power Sources 167 (2007) 258–264.
[8] Y.-M. Kim, P.K. Lohsoontorn, J. Bae, J. Power Sources 195 (2010) 6420–6427.
[9] J. Akedo, J. Am. Ceram. Soc. 89 (6) (2006) 1834–1839.
[10] J.-J. Choi, B.-D. Hahn, J. Ryu, W.-H. Yoon, B.-K. Lee, D.-S. Park, Sens. Actuators A 153 (1) (2009) 89–95.
[11] J.-J. Choi, B.-D. Hahn, J. Ryu, W.-H. Yoon, D.-S. Park, J. Appl. Phys. 102 (2007) 044101.
[12] H.-Y. Jung, S.-H. Choi, H. Kim, J.-W. Son, J. Kim, H.-W. Lee, J.-H. Lee, J. Power Sources 159 (2006) 478–483.
[13] H.-S. Noh, J.-W. Son, H.-R. Lee, H. Kim, J.-H. Lee, H.-W. Lee, J. Korean Ceram. Soc. 47 (2010) 75–81.
[14] J.-J. Choi, J. Ryu, B.-D. Hahn, W.-H. Yoon, B.-K. Lee, J.-H. Choi, D.-S. Park, J. Alloys Compd. 492 (1–2) (2010) 488–495.
[15] H.-S. Noh, J.-W. Son, H. Lee, H.-S. Song, H.-W. Lee, J.-H. Lee, J. Electrochem. Soc. 156 (2009) B1484–B1490.